J|A|C|S
ARTICLES

Published on Web 06/08/2009

A Five-Center Redox System: Molecular Coupling of Two Noninnocent Imino-*o*-benzoquinonato-Ruthenium Functions through a π Acceptor Bridge

Atanu Kumar Das,[†] Biprajit Sarkar,[†] Jan Fiedler,[‡] Stanislav Zális,[‡] Ingo Hartenbach,[†] Sabine Strobel,[†] Goutam Kumar Lahiri,[§] and Wolfgang Kaim*[,†]

Institut für Anorganische Chemie, Universität Stuttgart, Pfaffenwaldring 55, D-70550 Stuttgart, Germany, J. Heyrovský Institute of Physical Chemistry, v.v.i., Academy of Sciences of the Czech Republic, Dolejškova 3, CZ-18223 Prague, Czech Republic, and Department of Chemistry, Indian Institute of Technology, Bombay, Powai, Mumbai-400076, India

Received March 16, 2009; E-mail: kaim@iac.uni-stuttgart.de

Abstract: Combining the concepts of noninnocent behavior of metal/ligand entities and the coupling of redox-active moieties via an electronically mediating bridge led to the synthesis and the structural, electrochemical, and spectroscopic characterization of $[Cl(Q)Ru(\mu\text{-tppz})Ru(Q)Cl]^n$ where Q^o is 4,6-di-*tert*-butyl-*N*-phenyl-*o*-iminobenzoquinone and $tppz^o$ is 2,3,5,6-tetrakis(2-pyridyl)pyrazine, the available oxidation states being $Ru^{II,III,IV}$, $Q^{o,\bullet-,2-}$, and $tppz^{o,\bullet-,2-}$. One-electron transfer steps between the $n = (2-)$ and $(4+)$ states were studied by cyclic voltammetry and by EPR, UV−vis−NIR spectroelectrochemistry for the structurally characterized *anti* isomer of $[Cl(Q)Ru(\mu\text{-tppz})Ru(Q)Cl](PF_6)_2$, $\mathbf{2}(PF_6)_2$, the only configuration obtained. The combined investigations reveal that $\mathbf{2}^{2+}$ is best described as $[Cl(Q^{\bullet-})Ru^{III}(\mu\text{-}tppz^o)Ru^{III}(Q^{\bullet-})Cl]^{2+}$ with antiferromagnetic coupling between the ruthenium(III) and the iminosemiquinone components at each end. A metal-based spin as evident from large *g* factor anisotropy (EPR) and an intense intervalence absorption band at 1850 nm in the near-infrared (NIR) suggest that oxidation occurs at both iminosemiquinones to yield two $Ru^{II,III}$-bonded quinones, implying redox-induced electron transfer. Reduction takes place stepwise at the metal centers yielding iminosemiquinone complexes of $Ru^{III,II}$ as evident from radical complex EPR spectra with small $^{99,101}Ru$ hyperfine contributions. After complete metal reduction to ruthenium(II) the bridging ligand tppz is being reduced stepwise as apparent from typical NIR absorption bands around 1000 nm and from small *g* anisotropy of the monoanion $[Cl(Q^{\bullet-})Ru^{II}(\mu\text{-}tppz^{\bullet-})Ru^{II}(Q^{\bullet-})Cl]^-$. A structure-based DFT calculation confirms the Ru−Cl character of the HOMO and the iminoquinone-dominated LUMO and illustrates the orbital interaction pattern of the five electron transfer active components in this new system.

Introduction

Studies of the electronic interaction between electroactive transition metal centers via a molecular bridge have greatly contributed to our current understanding of redox reactivity[1,2] and of its potential in information transfer[3] and energy-relevant research.[4] The classical example of the Creutz−Taube ion **1**,[1] a delocalized mixed-valent diruthenium(III,II) species,[1] has stimulated a wide variety of theoretical,[5] methodical,[6] and conceptual advances.[7]

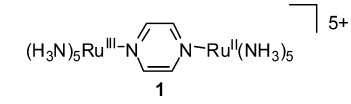

1

However, in this and many related cases the interacting centers are restricted to the metal ions so that a three-site arrangement, metal−bridge−metal (Scheme 1A), could be developed as an adequate description of the bridge-mediated

[†] Universität Stuttgart.
[‡] J. Heyrovský Institute of Physical Chemistry.
[§] Indian Institute of Technology, Bombay.

(1) Creutz, C. *Prog. Inorg. Chem.* **1983**, *30*, 1. (b) Richardson, D. E.; Taube, H. *Coord. Chem. Rev.* **1984**, *60*, 107. (c) Crutchley, R. J. *Adv. Inorg. Chem.* **1994**, *41*, 273. (d) Demadis, K. D.; Hartshorn, D. C; Meyer, T. J. *Chem. Rev.* **2001**, *101*, 2655.
(2) Salsman, J. C.; Kubiak, C. P.; Ito, T. *J. Am. Chem. Soc.* **2005**, *127*, 2382. (b) Londergan, C. H.; Salsman, J. C.; Lear, B. J.; Kubiak, C. P. *Chem. Phys.* **2006**, *324*, 57.
(3) Braun-Sand, S. B.; Wiest, O. *J. Phys. Chem. B* **2003**, *107*, 9624. (b) Braun-Sand, S. B.; Wiest, O. *J. Phys. Chem. A* **2003**, *107*, 285. (c) Wang, Y.; Lieberman, M. *IEEE Trans. Nanotech.* **2004**, *3*, 368. (d) Zhao, P.; Woolard, D.; Seminario, J. M.; Trew, R. *Int. J. High Speed Electronics* **2006**, *16*, 705.
(4) Heyduk, A. F.; Nocera, D. G. *Science* **2001**, *293*, 1639. (b) Esswein, A. J.; Veige, A. S.; Piccoli, P. M. B.; Schultz, A. J.; Nocera, D. G. *Organometallics* **2008**, *27*, 1073.
(5) Hush, N. S. *Prog. Inorg. Chem.* **1967**, *8*, 391. (b) Hush, N. S. *Coord. Chem. Rev.* **1985**, *64*, 135. (c) Creutz, C.; Newton, M. D.; Sutin, N. *J. Photochem. Photobiol. A* **1994**, *82*, 47.
(6) Petrov, V.; Hupp, J. T.; Mottley, C.; Mann, L. C. *J. Am. Chem. Soc.* **1994**, *116*, 2171. (b) Oh, D. H.; Sano, M.; Boxer, S. G. *J. Am. Chem. Soc.* **1991**, *113*, 6880. (c) Rocha, R. C.; Brown, M. G.; Londergan, C. H.; Salsman, J. C.; Kubiak, C. P.; Shreve, A. P. *J. Phys. Chem. A* **2005**, *109*, 9006.
(7) Prassides, K, Ed. *Mixed Valency Systems - Applications in Chemistry, Physics and Biology*; Kluwer Academic Publishers: Dordrecht, 1991. (b) Fabre, M.; Bonvoisin, J. *J. Am. Chem. Soc.* **2007**, *129*, 1434.

Scheme 1

(A) M-(μ-L)-M

(B) Q-M-(μ-L)-M-Q

μ-L = μ-tppz$^{o/\bullet-/2-}$; M = Ru$^{II/III/IV}$; Q = Q$^{o/\bullet-/2-}$

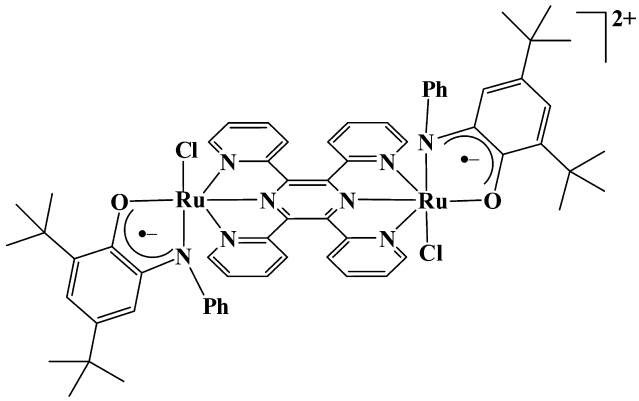

communication ("superexchange").[1,5,8] The role of the organic, frequently π-conjugated bridge has been probed by studying the effect of its variation[1,9] on the electrochemical and electronic coupling, i.e., on the splitting of redox waves at E_1 and E_2 for stepwise electron transfer (eq 1), and on the electronic transition to the "inter-valence" charge transfer (IVCT) excited state (eq 2).[1,2,7]

$$M^{(n)+}(\mu\text{-L})M^{(n)+} \overset{E_1}{\rightleftharpoons} M^{(n)+}(\mu\text{-L})M^{(n+1)+} \overset{E_2}{\rightleftharpoons} M^{(n+1)+}(\mu\text{-L})M^{(n+1)+} \quad (1)$$

$$M^{(n)+}(\mu\text{-L})M^{(n+1)+} \xrightarrow[\text{IVCT}]{h\nu} {}^{*}[M^{(n+1)+}(\mu\text{-L})M^{(n)+}] \quad (2)$$

The coupling of *reaction centers* consisting of more than one atom has been investigated by studying electron/atom transfer sequences[10] and in a recent, only partially successful attempt to couple two {Ru(NO)} entities via a conjugated bridge.[11] Herein we describe the mediated coupling of two substituted monoimino-*o*-benzoquinonato-ruthenium moieties Q^{n}Ru^m, Q^o = 4,6-di-*tert*-butyl-*N*-phenyl-*o*-iminobenzoquinone, with variable oxidation states of both the metal *and* the (noninnocent) quinonoid ligand;[12,13] the bis-tridentate 2,3,5,6-tetrakis(2-pyridyl)pyrazine, μ-tppz, served as the molecular bridge[14,15] in [(Q)ClRu(μ-tppz)RuCl(Q)](PF$_6$)$_2$, **2**(PF$_6$)$_2$, containing the five-component redox system [Q^n-Ru^m-(μ-tppz^x)-Ru$^{m'}$-Q$^{n'}$] (Scheme 1B).

Tppz is known as a π accepting and thus also potentially noninnocent bis-tridentate bridge in dinuclear radical, mixed-valent, and other paramagnetic compounds[14] and in charge conducting coordination polymers.[15] On the other hand, the combination between ruthenium and quinone-type ligands has received much attention for the following reasons:

(1) exceptional metal-to-ligand charge-transfer interaction (back-donation)[12,16] and the ambiguity of oxidation state assignments,[17−21]
(2) stability and EPR accessibility of ruthenium(II)-semiquinone complexes[19] and their nontrivial electronic structure,[20]
(3) antiferromagnetic coupling between Ru^{III} and semiquinone radicals,[21]
(4) possible stabilization of coordinated radicals,[22] and
(5) the potential use of such dinuclear systems in water oxidation catalysis.[23]

Experimental Section

Instrumentation. EPR spectra in the X band were recorded with a Bruker System EMX. ^{1}H NMR spectra were taken on a Bruker AC 250 spectrometer. UV−vis−NIR absorption spectra

(8) Hupp, J. T. In *Comprehensive Coordination Chemistry II*; McCleverty, J. A., Meyer, T. J., Eds.; Elsevier Science: Amsterdam, 2003; p 709. (b) Crutchley, R. J. In *Comprehensive Coordination Chemistry II*; McCleverty, J. A., Meyer, T. J., Eds.; Elsevier Science: Amsterdam, 2003; p 235.
(9) Kaim, W.; Klein, A.; Glöckle, M. *Acc. Chem. Res.* **2000**, *33*, 755. (b) Kaim, W.; Sarkar, B. *Coord. Chem. Rev.* **2007**, *251*, 584. (c) Kaim, W.; Lahiri, G. K. *Angew. Chem.* **2007**, *119*, 1808; *Angew. Chem., Int. Ed.* **2007**, *46*, 1778.
(10) Baumann, F.; Kaim, W.; Denninger, G.; Kümmerer, H. J.; Fiedler, J. *Organometallics* **2005**, *24*, 1966. (b) Kaim, W. In *New Trends in Molecular Electrochemistry*; Pombeiro, A. J. L., Ed.; Fontis Media: Lausanne, 2004; p 127.
(11) Singh, P.; Sieger, M.; Fiedler, J.; Su, C.-Y.; Kaim, W. *Dalton Trans.* **2008**, 868.
(12) Haga, M.; Dodsworth, E. S.; Lever, A. B. P. *Inorg. Chem.* **1986**, *25*, 447. (b) Masui, H.; Lever, A. B. P.; Auburn, P. *Inorg. Chem.* **1991**, *30*, 2402. (c) Ebadi, M.; Lever, A. B. P. *Inorg. Chem.* **1999**, *38*, 467. (d) Lever, A.B. P.; Auburn, P. R.; Dodsworth, E. S.; Haga, M.; Liu, W.; Melnik, M.; Nevin, W. A. *J. Am. Chem. Soc.* **1988**, *110*, 8076. (e) Auburn, P. R.; Dodsworth, E. S.; Haga, M.; Liu, W.; Nevin, W. A.; Lever, A. B. P. *Inorg. Chem.* **1991**, *30*, 3502. (f) Poddel'sky, A. I.; Cherkasov, V. K.; Abakumov, G. A. *Coord. Chem. Rev.* **2009**, *253*, 291.
(13) Chaudhuri, P.; Verani, C. N.; Bill, E.; Bothe, E.; Weyhermüller, T.; Wieghardt, K. *J. Am. Chem. Soc.* **2001**, *123*, 2213.
(14) Chanda, N.; Sarkar, B.; Fiedler, J.; Kaim, W.; Lahiri, G. K. *Inorg. Chem.* **2004**, *43*, 5128. (b) Ghumaan, S.; Sarkar, B.; Chanda, N.; Sieger, M.; Fiedler, J.; Kaim, W.; Lahiri, G. K. *Inorg. Chem.* **2006**, *45*, 7955. (c) Koley, M.; Sarkar, B.; Ghumaan, S.; Bulak, E.; Fiedler, J.; Kaim, W.; Lahiri, G. K. *Inorg. Chem.* **2007**, *46*, 3736. (d) Rocha, R. C.; Rein, F. M.; Jude, H.; Shreve, A. P.; Concepcion, J. J.; Meyer, T. J. *Angew. Chem.* **2008**, *120*, 513; *Angew. Chem., Int. Ed.* **2008**, *47*, 503. (e) Chanda, N.; Laye, R. H.; Chakraborty, S.; Paul, R. L.; Jeffery, J. C.; Ward, M. D.; Lahiri, G. K. *J. Chem. Soc., Dalton Trans.* **2002**, 3496. (f) Carranza, J.; Sletten, J.; Brennan, C.; Lloret, F.; Cano, J.; Julve, M. *Dalton Trans.* **2004**, 3997.
(15) Fantacci, S.; De Angelis, F.; Wang, J.; Bernhard, S.; Selloni, A. *J. Am. Chem. Soc.* **2004**, *126*, 9715. (b) Flores-Torres, S.; Hutchison, G. R.; Soltzberg, L. J.; Abruña, H. D. *J. Am. Chem. Soc.* **2006**, *126*, 1513.
(16) Kalinina, D.; Dares, C.; Kaluarachchi, H.; Potvin, P. G.; Lever, A. B. P. *Inorg. Chem.* **2008**, *47*, 10110.
(17) Ernst, S.; Hänel, P.; Jordanov, J.; Kaim, W.; Kasack, V.; Roth, E. *J. Am. Chem. Soc.* **1989**, *111*, 1733. (b) Schwederski, B.; Kasack, V.; Kaim, W.; Roth, E.; Jordanov, J. *Angew. Chem.* **1990**, *102*, 74; *Angew. Chem., Int. Ed. Engl.* **1990**, *29*, 78. (c) Ernst, S.; Kasack, V.; Bessenbacher, C.; Kaim, W. *Z. Naturforsch.* **1987**, *42b*, 425.
(18) Patra, S.; Sarkar, B.; Mobin, S. M.; Kaim, W.; Lahiri, G. K. *Inorg. Chem.* **2003**, *42*, 6469.
(19) Kaim, W.; Ernst, S.; Kasack, V. *J. Am. Chem. Soc.* **1990**, *112*, 173. (b) Waldhör, E.; Schwederski, B.; Kaim, W. *J. Chem. Soc., Perkin Trans. 2* **1993**, 2109. (c) Ye, S.; Sarkar, B.; Duboc, C.; Fiedler, J.; Kaim, W. *Inorg. Chem.* **2005**, *44*, 2843.
(20) Remenyi, C.; Kaupp, M. *J. Am. Chem. Soc.* **2005**, *127*, 11399.
(21) Maji, S.; Sarkar, B.; Mobin, S. M.; Fiedler, J.; Urbanos, F. A.; Jimenez-Aparicio, R.; Kaim, W.; Lahiri, G. K. *Inorg. Chem.* **2008**, *47*, 5204. (b) Ghumaan, S.; Sarkar, B.; Maji, S.; Puranik, V. G.; Fiedler, J.; Urbanos, F. A.; Jimenez-Aparicio, R.; Kaim, W.; Lahiri, G. K. *Chem.—Eur. J.* **2008**, *14*, 10816. (c) Mitra, K. N.; Peng, S.-M.; Goswami, S. *Chem. Commun.* **1998**, 1685. (d) Bill, E.; Bothe, E.; Chaudhuri, P.; Chlopek, K.; Herbian, D.; Kokatam, S.; Ray, K.; Weyhermüller, T.; Neese, F.; Wieghardt, K. *Chem.—Eur. J.* **2005**, *11*, 204.
(22) Kobayashi, K.; Ohtsu, H.; Wada, T.; Kato, T.; Tanaka, K. *J. Am. Chem. Soc.* **2003**, *125*, 6729. (b) Miyazato, Y.; Wada, T.; Muckerman, J. T.; Fujita, E.; Tanaka, K. *Angew. Chem.* **2007**, *119*, 5830; *Angew. Chem., Int. Ed.* **2007**, *46*, 5728.
(23) Muckerman, J. T.; Polyansky, D. E.; Wada, T.; Tanaka, K.; Fujita, E. *Inorg. Chem.* **2008**, *47*, 1787.

were recorded on J&M TIDAS and Shimadzu UV 3101 PC spectrophotometers. Cyclic voltammetry was carried out in 0.1 M Bu_4NPF_6 solutions using a three-electrode configuration (glassy carbon working electrode, Pt counter electrode, Ag/AgCl reference) and a PAR 273 potentiostat and function generator. The ferrocene/ferrocenium (Fc/Fc^+) couple served as internal reference. Spectroelectrochemistry was performed using an optically transparent thin-layer electrode (OTTLE) cell.[24] A two-electrode capillary served to generate intermediates for X band EPR studies.[19]

Materials. The precursor complex $Cl_3Ru(\mu\text{-tppz})RuCl_3$ was prepared according to a reported procedure.[25] The ligand 2-anilino-4,6-di-*tert*-butylphenol was prepared as reported.[13]

Synthesis of 2(PF$_6$)$_2$. The precursor complex $Cl_3Ru(\mu\text{-tppz})RuCl_3$ (100 mg, 0.12 mmol) and 2-anilino-4,6-di-*tert*-butylphenol (L, 79 mg, 0.26 mmol) were refluxed for 6 h in 20 mL of ethanol in the presence of excess LiCl (52 mg, 1.2 mmol) and CH_3COONa (25 mg, 0.30 mmol). The initial light green solution changed to deep green. After removal of the solvent the residue was dissolved in 5 mL of an acetonitrile/methanol (4/1) mixture, and an excess of a saturated aqueous solution of NH_4PF_6 was added. The precipitate thus obtained was collected and washed with ice-cold water. The crude product was purified by column chromatography (neutral alumina). The complex **2**$(PF_6)_2$ was eluted as a green zone using a CH_2Cl_2/CH_3CN mixture (5/3) as eluent. Yield: 40% (76 mg). λ_{max}/nm (ϵ/$M^{-1}cm^{-1}$): 234 (20340), 378 (14850), 489 (sh), 684 (28750). $C_{64}H_{66}Cl_2F_{12}N_8O_2P_2Ru_2$ (1542.27): Calcd C, 49.84; H, 4.31; N, 7.27. Found: C, 50.03; H, 4.40; N, 7.17%. A positive ion electrospray mass spectrum of $\mathbf{2}^{2+}$ in CH_3CN exibited signals at $m/z = 626.15$, corresponding to $\mathbf{2}^{2+}/2$ (calculated molecular mass/2, 626.16). ^{1}H NMR (CD_2Cl_2, δ(*J*/Hz)): 8.25 (t, 7.9, 7.9), 7.97 (s), 7.86 − 7.69 (m), 7.52 (d, 7.8), 7.16 − 6.98 (m), 6.82 (t, 7.8, 7.2), 6.5 (s), 1.17 (s), 1.89 (s).

X-ray Crystallography. Single crystals were obtained as **2**$(PF_6)_2\cdot(C_7H_8)$ from acetonitrile/toluene via the diffusion method. All crystals investigated had the same unit cell, and the best data were used for refinement. Data were collected of selected specimens with a NONIUS Kappa CCD diffractometer at 100 K. The structure was solved using direct methods with refinement by full-matrix least-squares of F^2, employing the program system SHELXL 97 in connection with absorption correction.[26,27] All non-hydrogen atoms were refined anisotropically; hydrogen atoms were introduced at appropriate positions.

DFT Calculations. The electronic structures of $[Cl(Q)Ru(\mu\text{-tppz})Ru(Q)Cl]^{n+}$ ($n = 1, 2, 3$) were calculated by the density functional theory (DFT) method using the Gaussian 03[28] and ADF2008.01[29] program packages using the experimental (crystal) structure of **2**$(PF_6)_2$. Electronic transitions were calculated by the time-dependent DFT (TD DFT) method.

The hybrid functional of Perdew, Burke, and Ernzerhof[30] (PBE0) was used within Gaussian (G03/PBE0) together with 6-31G* polarized double-ζ basis sets[31] for C, N, H, and O atoms and effective core pseudopotentials and corresponding optimized sets of basis functions for the Ru atoms.[32] The solvent was described by the polarizable conductor calculation model (CPCM)[33] in TD DFT calculations.

Slater type orbital (STO) basis sets of triple-ζ quality with two polarization functions for the Ru atom and of triple-ζ quality with one polarization function for the remaining atoms were employed within ADF2008.01. The inner shells were represented by the frozen core approximation (1s for C, N, O, 1s-3d for Ru were kept frozen). The calculations were done with the functional including Becke's gradient correction to the local exchange expression in conjunction with Perdew's gradient correction to the local correlation (ADF/BP).[34] The scalar relativistic (SR) zero-order regular approximation (ZORA) was used within ADF calculations. The *g* tensor was obtained from a spin-nonpolarized wave function after incorporating the spin−orbit (SO) coupling. *A* and *g* tensors were obtained by first-order perturbation theory from a ZORA Hamiltonian in the presence of a time-independent magnetic field.[35] Core electrons were included in calculations of *A* tensors.

Table 1. Crystallographic Data for **2**$(PF_6)_2\cdot(C_7H_8)$

empirical formula	$C_{78}H_{82}Cl_2F_{12}N_8O_2P_2Ru_2$
fw	1726.50
T (K)	100(1)
λ (Å)	0.710 73
crystal system	triclinic
space group	$P\bar{1}$
Z	1
a (Å)	12.660(1)
b (Å)	13.224(1)
c (Å)	12.9492(9)
α (deg)	81.382(5)
β (deg)	62.819(6)
γ (deg)	76.633(5)
V (Å^3)	1873.8(3)
ρ_{calcd} (g cm^{-3})	1.530
μ (mm^{-1})	0.600
θ range (deg)	3.06−21.96
collected data	8434
unique data/R_{int}	4509/0.141
no. of data > 4σ	2700
no. of parameters	444
GOF[a]	1.012
R1, wR2 ($I > 4\sigma$)[b]	0.0656, 0.1161
resd dens (e/Å^3)	0.508/−0.732

[a] GOF = $\{\Sigma[w(F_o^2 - F_c^2)^2]/(n - p)\}^{1/2}$, where n and p denote the number of data and parameters. [b] R1 = $\Sigma(||F_o| - |F_c||)/\Sigma|F_o|$ and wR2 = $\{\Sigma[w(F_o^2 - F_c^2)^2]/\Sigma[w(F_o^2)^2]\}^{1/2}$ where $w = 1/[\sigma^2(F_o^2) + (a\cdot P)^2 + b\cdot P]$ and $P = [(\text{Max}; 0, F_o^2) + 2\cdot F_c^2]/3$.

Results and Discussion

Structure and Electrochemistry. The green complex $[Cl(Q)Ru(\mu\text{-tppz})Ru(Q)Cl](PF_6)_2$, **2**$(PF_6)_2$, shows the presence of only one of the two possible positional isomers (*syn*, *anti*) through ^{1}H NMR spectroscopy. The crystal structure analysis reveals the *anti* isomer (Tables 1, 2 and Figure 1) and an unreduced tppz bridge.[36,39] Despite the limited crystal quality and refinement results, the data allowed us to identify two peripheral 4,6-di-*tert*-butyl-*N*-phenyl-*o*-benzosemiquinonato ligands according

(24) Krejèik, M.; Danek, M.; Hartl, F. *J. Electroanal. Chem. Interfacial Electrochem.* **1991**, *317*, 179.
(25) Hartshorn, C. M.; Daire, N.; Tondreau, V.; Loeb, B.; Meyer, T. J.; White, P. S. *Inorg. Chem.* **1999**, *38*, 3200.
(26) Sheldrick, G. M. Program for Crystal Structure Solution and Refinement; Universität Göttingen, 1997.
(27) Herrendorf, W.; Bärnighausen, H. *Program HABITUS; Karlsruhe*; Germany, 1993.
(28) Frisch, M. J.; Trucks, G.; Schlegel, H. B. et al. *Gaussian 03*, revision C.02; Gaussian, Inc.: Wallingford, CT; 2004.
(29) te Velde, G.; Bickelhaupt, F. M.; van Gisbergen, S. J. A.; Fonseca Guerra, C.; Baerends, E. J.; Snijders, J. G.; Ziegler, T. *J. Comput. Chem.* **2001**, *22*, 931. (b) ADF 2008 01, SCM, Theoretical Chemistry, Vrije Universiteit, Amsterdam, The Netherlands, http://www.scm.com.
(30) Perdew, J. P.; Burke, K.; Ernzerhof, M. *Phys. Rev. Lett.* **1996**, *77*, 3865.
(31) Hariharan, P. C.; Pople, J. A. *Theor. Chim. Acta* **1973**, *28*, 213.
(32) Andrae, D.; Häussermann, U.; Dolg, M.; Stoll, H.; Preuss, H. *Theor. Chim. Acta* **1990**, *77*, 123.
(33) Cossi, M.; Rega, N.; Scalmani, G.; Barone, V. *J. Comput. Chem.* **2003**, *24*, 669.
(34) Becke, A. D. *Phys. Rev. A* **1988**, *38*, 3098. (b) Perdew, J. P.; Wang, Y. *Phys. Rev. B* **1992**, *45*, 13244.
(35) van Lenthe, E.; van der Avoird, A.; Wormer, P. E. S. *J. Chem. Phys.* **1997**, *107*, 2488. (b) van Lenthe, E.; van der Avoird, A.; Wormer, P. E. S. *J. Chem. Phys.* **1998**, *108*, 4783.

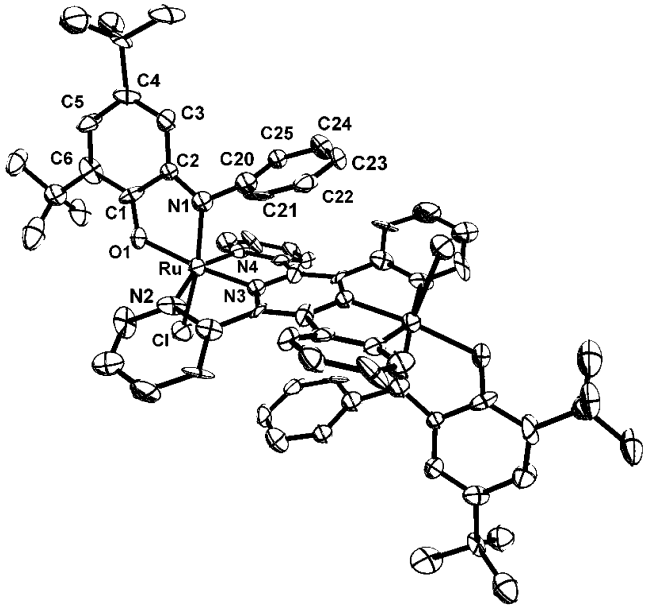

Figure 1. Molecular structure of $[(Q)ClRu(\mu\text{-tppz})RuCl(Q)]^{2+}$ in the crystal of $\mathbf{2}(PF_6)_2\cdot(C_7H_8)$.

to established structure criteria[37] such as the intermediate C—O and C═C(meta) distances.

Specifically, the oxidation state assignment $[(Q^{\bullet-})\text{-}Ru^{III}\text{-}(\mu\text{-tppz}^{o})\text{-}Ru^{III}\text{-}(Q^{\bullet-})]$ follows from the fit with statistically derived bond parameters for *o*-C_6H_4XY ligands which arrived at 1.30, 1.35, and 1.36 Å for the CO, CNH, and C═C(meta) bonds in *o*-iminobenzosemiquinones, respectively.[37] The C═C(meta) bond is most sensitive among the intraring C—C bonds because it clearly shows the transition from a short double bond value in the quinone form (alternating bonds) to an "aromatic" C—C bond of bond order 1.5 in the fully reduced state. The corresponding experimental values for $\mathbf{2}^{2+}$ are 1.292(11), 1.321(11), and 1.374(11) Å, respectively. The observed diamagnetism and the semiquinone assignment for Q imply strong antiferromagnetic coupling between $Q^{\bullet-}$ ($S = {}^1/_2$) and coordinated Ru^{III} ($S = {}^1/_2$) on either side of $\mathbf{2}^{2+}$.[21] The N-phenyl substituents of the iminosemiquinone ligands and the central pyrazine ring of the tppz bridge exhibit a $\pi/\pi/\pi$ "triple-decker" stacking interaction[14e,38] (Figure 1) with N3—C20 as the shortest distance at 2.993 Å; the distance between the pyrazine-bridged[39] metal ions is 6.544 Å.

The thus characterized dicationic form can be oxidized in two reversible steps and reduced in four reversible steps; a fifth, partially reversible reduction wave was also detected (Figure 2, Table 3, Scheme 2). EPR and UV—vis—NIR spectroelectrochemistry (Table 4) were used to analyze the electron configuration for these six additional redox states. Scheme 2 summarizes the alternatives and lists our preferred interpretation in the left-hand column.

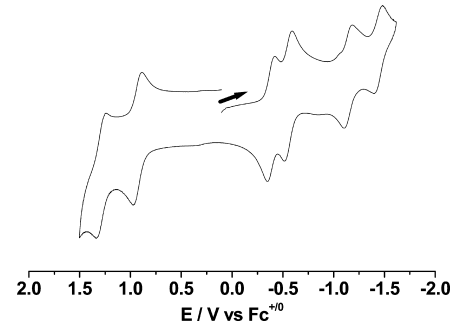

Figure 2. Cyclic voltammogram of $\mathbf{2}(PF_6)_2$ in CH_3CN/0.1 M Bu_4NPF_6.

Table 2. Selected Bond Lengths (Å) and Angles (deg) for $\mathbf{2}(PF_6)_2\cdot(C_7H_8)$

Ru—N1	1.993(8)
Ru—N2	2.040(7)
Ru—N3	1.936(7)
Ru—N4	2.047(7)
Ru—O1	2.020(6)
Ru—Cl	2.387(3)
O1—C 1	1.292(11)
N1—C2	1.321(11)
C6—C5	1.379(13)
C5—C4	1.469(13)
C4—C3	1.369(12)
C1—C2	1.460(12)
C3—C2	1.430(13)
C1—C6	1.433(13)
N1—Ru—Cl	167.3(2)
N2—Ru—N4	156.2(3)
N3—Ru—O1	171.2(3)
N2—Ru—N3	80.0(3)
N3—Ru—N4	79.1(3)
N4—Ru—O1	103.6(3)
N4—Ru—N1	90.3(3)
N2—Ru—N1	102.5(3)
O1—Ru—N1	77.4(3)
O1—Ru—N2	98.8(3)
O1—Ru—N4	103.6(3)
O1—C1—C2	114.7(8)
C1—C2—N1	112.5(9)
C2—N1—Ru	117.8(6)

Oxidation. Oxidation of diamagnetic, EPR-silent $\mathbf{2}^{2+}$ results in the appearance of a rhombic EPR signal (Figure 3A, $g_1 = 2.643$, $g_2 = 2.101$, $g_3 = 1.785$) at 110 K in CH_3CN/0.1 M Bu_4NPF_6 (no signal at 295 K) as is typical for distorted ruthenium(III) in its low-spin d^5 configuration.[40] Although several alternatives as given in Scheme 2 would explain this EPR result, the emergence and subsequent disappearance (on second oxidation) of an intense near-infrared band at 1853 nm ($\epsilon = 4150\ M^{-1}\ cm^{-1}$, $\Delta\nu_{1/2} = 1350\ cm^{-1}$) on spectroelectrochemical oxidation in CH_3CN/0.1 M Bu_4NPF_6 (Figure 4) strongly suggest a mixed-valent configuration $[Cl(Q^{o})Ru^{II}(\mu\text{-tppz})Ru^{III}(Q^{o})Cl]^{3+}$ with a low-energy IVCT transition and a sizable comproportionation constant of $10^{6.1}$ (complex **1** has $K_c = 10^{7.3}$ in acetonitrile; $\lambda_{max} = 1600$ nm, $\epsilon = 5000\ M^{-1}\ cm^{-1}$, $\Delta\nu_{1/2} = 1400\ cm^{-1}$ in water).[1,41] The *reduction* of one ruthenium(III) center from the initial configuration $[Cl(Q^{\bullet-})Ru^{III}(\mu\text{-tppz})Ru^{III}(Q^{\bullet-})Cl]^{2+}$ of $\mathbf{2}^{2+}$ on *oxidation* to

(36) Reduced pyrazines exhibit characteristic CC bond shortening and CN bond lengthening. (a) Kaim, W. *Rev. Chem. Intermed.* **1987**, *8*, 247. (b) Kaim, W.; Schulz, A.; Hilgers, F.; Hausen, H.-D.; Moscherosch, M.; Lichtblau, A.; Jordanov, J.; Roth, E.; Zalis, S. *Res. Chem. Intermed.* **1993**, *19*, 603.

(37) Kokatam, S.; Weyhermüller, Th.; Bothe, E.; Chaudhuri, P.; Wieghardt, K. *Inorg. Chem.* **2005**, *44*, 3709. (b) Bhattacharya, S.; Gupta, P.; Basuli, F.; Pierpont, C. G. *Inorg. Chem.* **2002**, *41*, 5810.

(38) For a related example, see: Sieger, M.; Vogler, C.; Klein, A.; Knödler, A.; Wanner, M.; Fiedler, J.; Zalis, S.; Snoeck, T. L.; Kaim, W. *Inorg. Chem.* **2005**, *44*, 4637.

(39) Kaim, W. *Angew. Chem.* **1983**, *95*, 201; *Angew. Chem., Int. Ed. Engl.* **1983**, *22*, 171.

(40) Poppe, J.; Moscherosch, M.; Kaim, W. *Inorg. Chem.* **1993**, *32*, 2640.

(41) Creutz, C.; Chou, M. H. *Inorg. Chem.* **1987**, *26*, 2995.

Scheme 2

E (V)	K_c	assigned oxidation state distribution		alternative(s)
		$[ClQ^{o}Ru^{III}(\mu\text{-tppz})Ru^{III}Q^{o}Cl]^{4+}$	or	$[ClQ^{\bullet}Ru^{IV}(\mu\text{-tppz})Ru^{IV}Q^{\bullet}Cl]^{4+}$
1.29		$-e^{-}\ \|\ +e^{-}$		
	$10^{6.1}$	$[ClQ^{o}Ru^{II}(\mu\text{-tppz})Ru^{III}Q^{o}Cl]^{3+}$	or	$[ClQ^{o}Ru^{III}(\mu\text{-tppz})Ru^{III}Q^{\bullet}Cl]^{3+}$
0.93		$-e^{-}\ \|\ +e^{-}$	or	$[ClQ^{\bullet}Ru^{IV}(\mu\text{-tppz})Ru^{III}Q^{\bullet}Cl]^{3+}$
		$[ClQ^{\bullet}Ru^{III}(\mu\text{-tppz})Ru^{III}Q^{\bullet}Cl]^{2+}$		
-0.38		$-e^{-}\ \|\ +e^{-}$		
	$10^{2.9}$	$[ClQ^{\bullet}Ru^{II}(\mu\text{-tppz})Ru^{III}Q^{\bullet}Cl]^{+}$	or	$[ClQ^{\bullet}Ru^{III}(\mu\text{-tppz}^{\bullet-})Ru^{III}Q^{\bullet}Cl]^{+}$
-0.55		$-e^{-}\ \|\ +e^{-}$	or	$[ClQ^{2-}Ru^{III}(\mu\text{-tppz})Ru^{III}Q^{\bullet}Cl]^{+}$
		$[ClQ^{\bullet}Ru^{II}(\mu\text{-tppz})Ru^{II}Q^{\bullet}Cl]$	or	$[ClQ^{\bullet}Ru^{III}(\mu\text{-tppz}^{2-})Ru^{III}Q^{\bullet}Cl]$
-1.15		$-e^{-}\ \|\ +e^{-}$	or	$[ClQ^{2-}Ru^{III}(\mu\text{-tppz})Ru^{III}Q^{2-}Cl]$
	$10^{4.9}$	$[ClQ^{\bullet}Ru^{II}(\mu\text{-tppz}^{\bullet-})Ru^{II}Q^{\bullet}Cl]^{-}$	or	$[ClQ^{2-}Ru^{II}(\mu\text{-tppz})Ru^{II}Q^{\bullet}Cl]^{-}$
-1.44		$-e^{-}\ \|\ +e^{-}$		
		$[ClQ^{\bullet}Ru^{II}(\mu\text{-tppz}^{2-})Ru^{II}Q^{\bullet}Cl]^{2-}$	or	$[ClQ^{2-}Ru^{II}(\mu\text{-tppz})Ru^{II}Q^{2-}Cl]^{2-}$
-1.86		$-e^{-}\ \|\ +e^{-}$		

Table 3. Redox Potentials for $\mathbf{2}(PF_6)_2$ from Cyclic Voltammetry

E/V (ΔE/mV) vs $Fc^{o/+}$ [a]					
ox 1	ox 2	red 1	red 2	red 3	red 4
+1.29 (80)	+0.93 (85)	−0.38 (70)	−0.55 (80)	−1.15 (74)	−1.44 (90)

[a] In CH_3CN/0.1 M Bu_4NPF_6, 100 mV/s, 298 K.

Table 4. Absorption Data for $\mathbf{2}^{n}$

complex[a]	λ/nm (ϵ/M^{-1} cm^{-1})
$\mathbf{2}^{4+}$	390 (14 960), 601 (11 090)
$\mathbf{2}^{3+}$	379 (13 590), 512 (sh), 622 (12 780), 1853 (4150)
$\mathbf{2}^{2+}$	378 (14 850), 489 (sh), 684 (28 750)
$\mathbf{2}^{1+}$	365 (15 770), 683 (16 970)
$\mathbf{2}^{0}$	306 (15 600), 358 (16 730), 750 (18 900), 1033 (sh)
$\mathbf{2}^{-}$	306 (13 890), 383 (14 250), 750 (13 760), 960 (sh)
$\mathbf{2}^{2-}$	356 (16 220), 730 (6200), 956 (sh), 1190 (sh)

[a] From spectroelectrochemistry in CH_3CN/0.1 M Bu_4NPF_6.

$\mathbf{2}^{3+}$ is made possible through the 2-fold oxidation of the iminosemiquinone to the iminoquinone state.

Such "oxidation-leading-to-reduction" mechanisms, also addressed as "redox-induced electron transfer" (RIET),[42] have raised attention in the context of mixed-valency[1,9] and valence tautomerism.[43] Some salient examples have been reviewed very recently,[42] and another example involving group 8 metal coordination chemistry of singlet diradical species has been reported.[44] The reverse pattern, a "reduction-leading-to-oxidation" mechanism, also based on intramolecular valence redistribution, has also been discussed for oligonuclear ruthenium complexes.[45]

The second oxidation to $\mathbf{2}^{4+}$ is likely to produce $[Cl(Q^{o})Ru^{III}(\mu\text{-tppz})Ru^{III}(Q^{o})Cl]^{4+}$; all three forms $\mathbf{2}^{2+}$, $\mathbf{2}^{3+}$, and $\mathbf{2}^{4+}$ exhibit an intense ($\epsilon > 10\,000$ M^{-1} cm^{-1}) MLCT/LLCT charge transfer band (Ru, $Q^{\bullet-}\rightarrow\pi^{*}$(tppz)) at 600−700 nm.

The composition of frontier orbitals as listed in Table S1 and depicted in Figure S1 and the qualitative DFT-calculated MO energy diagram of $\mathbf{2}^{2+}$ in Figure S2 show that the highest occupied molecular orbital (HOMO) (Figure S1) is predominantly centered at the Ru−Cl moieties and that the lower lying occupied orbitals have also mainly ruthenium character. The set of two energetically close lowest lying unoccupied MOs (LUMOs) with large contributions from π^{*}_{Q} orbitals is followed by two nearly degenerate π^{*}_{tppz} based unoccupied orbitals. Using this information and TD DFT methodology, the intense absorption at 684 nm in $\mathbf{2}^{2+}$ can be assigned to an MLCT transition from the HOMO to the LUMO+2 (Table S2). Figure 5 confirms that the DFT calculated spin density

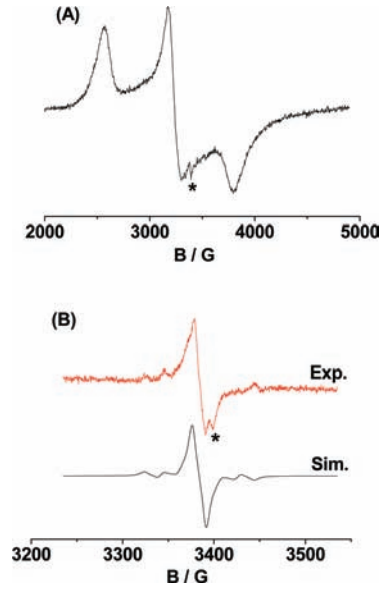

Figure 3. EPR spectra of electrogenerated $\mathbf{2}^{3+}$ (A, 110 K) and $\mathbf{2}^{+}$ (B, 295 K) in CH_3CN/0.1 M Bu_4NPF_6 (*: cavity signal).

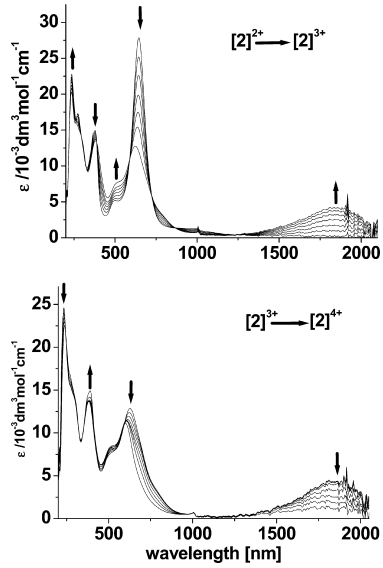

Figure 4. UV/vis/NIR-Spectroelectrochemical response of system $\mathbf{2}^{2+}$ on oxidation in CH_3CN/0.1 M Bu_4NPF_6.

(42) Miller, J. S.; Min, K. S. *Angew. Chem.* **2008**, *121*, 268; *Angew. Chem., Int. Ed.* **2008**, *48*, 262.
(43) (a) Evangelio, E.; Ruiz.-Molina, D. *Eur. J. Inorg. Chem.* **2005**, 2957. (b) Sato, O.; Cui, A.; Matsuda, R.; Tao, J.; Hayami, S. *Acc. Chem. Res.* **2007**, *40*, 361. (c) Dei, A.; Gatteschi, D.; Sangregorio, C.; Sorace, L. *Acc. Chem. Res.* **2004**, *37*, 827. (d) Hendrickson, D. N.; Pierpont, C. G. *Top. Curr. Chem.* **2004**, *234*, 63.
(44) Samanta, S.; Singh, P.; Fiedler, J.; Zalis, S.; Kaim, W.; Goswami, S. *Inorg. Chem.* **2008**, *47*, 1625.

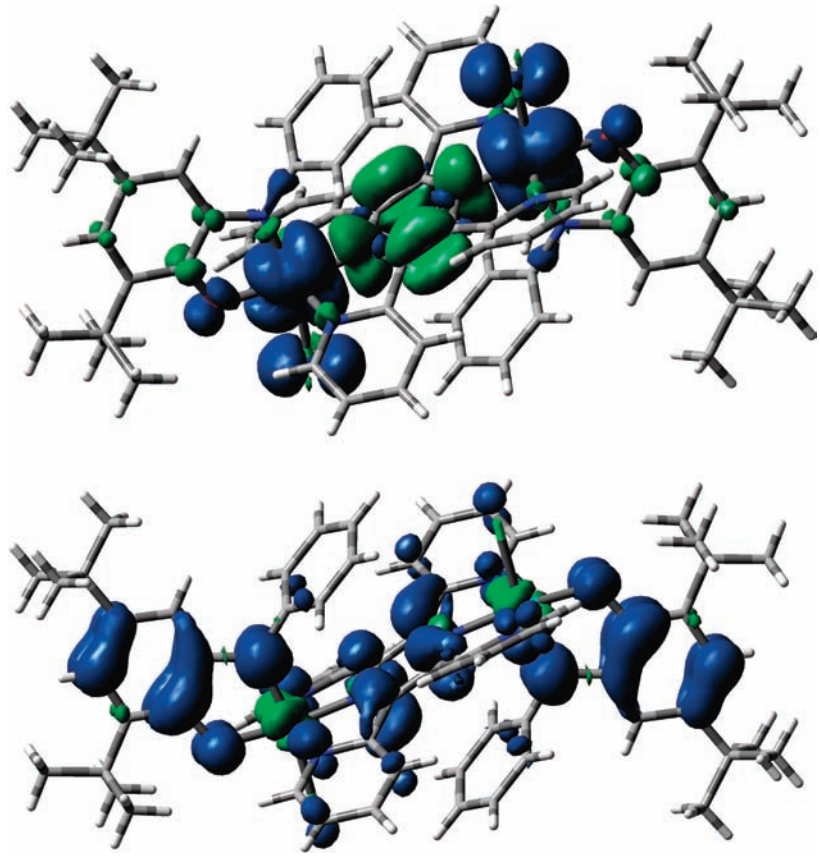

Figure 5. DFT calculated spin densities of $\mathbf{2}^{3+}$ (top) and $\mathbf{2}^{+}$ (bottom).

in $\mathbf{2}^{3+}$ is mainly localized on the metal centers, with some contribution from Cl and the slightly negative spin density on the tppz bridging ligand. G03/PBE0 calculations yield cumulated spin densities of 1.116, 0.186, and −0.280 for Ru, Cl, and tppz, respectively. No significant spin density was calculated for the Q ligands in $\mathbf{2}^{3+}$.

Reduction. The reduction sequence of $\mathbf{2}^{2+}$ starts with the EPR detected formation of an *o*-monoiminosemiquinone radical species ($g_{iso} = 2.0015$) coordinated to *one* ruthenium center with hyperfine coupling from ^{14}N ($I = 1$, 99.63%) at 0.50 mT (1 N) and from ^{99}Ru ($I = {}^5/_2$, 12.7%) and ^{101}Ru ($I = {}^5/_2$, 17.0%) at ∼2.1 mT (1 Ru).[18,46] Figure 3B confirms this analysis which implies reduction of one ruthenium(III) ion and formation of $[Cl(Q^{\bullet-})Ru^{II}(\mu\text{-tppz})Ru^{III}(Q^{\bullet-})Cl]^+$; the reduction of reducible[14e,15] tppz would produce $[Cl(Q^{\bullet-})Ru^{III}(\mu\text{-tppz}^{\bullet-})Ru^{III}(Q^{\bullet-})Cl]^+$ and an EPR spectrum with hyperfine coupling to two (pyrazine)N and to two Ru centers.

The closely following second reduction (comproportionation constant $K_c = 10^{2.9}$ for the $\mathbf{2}^{+}$ intermediate) shows a similar bathochromic shift of the charge transfer band as the first reduction (Figure 6) and an EPR spectrum (Figure 7) at $g_{iso} = 2.0033$ with $a(^{14}\text{N}) = 0.75$ mT (1 N) and $a(^{99,101}\text{Ru}) = 1.35$ mT (1 Ru). No triplet features (half-field EPR signal) were observed for the neutral $[Cl(Q^{\bullet-})Ru^{II}(\mu\text{-tppz})Ru^{II}(Q^{\bullet-})Cl]$, indicating little magnetic interaction between the iminosemiquinone radicals separated by $[ClRu(\mu\text{-tppz})RuCl]^{2+}$. The smaller metal hyperfine coupling and larger iminosemiquinone-N coupling constant in the doubly reduced species reflect different spin shifts which result from a balanced situation in the neutral compound as compared to a more polarized situation

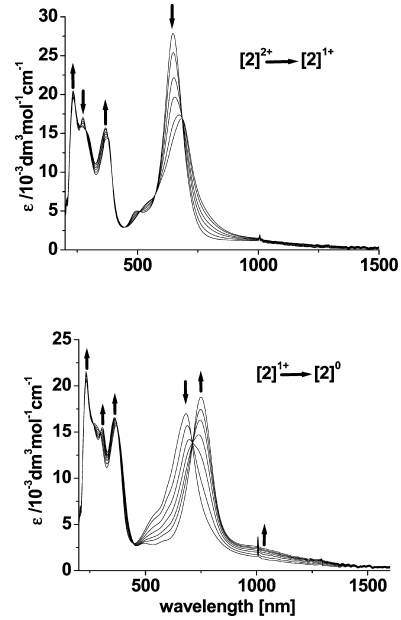

Figure 6. UV/vis/NIR-Spectroelectrochemical response of system $\mathbf{2}^{2+}$ on reduction in CH_3CN/0.1 M Bu_4NPF_6 (first two steps).

(45) Moscherosch, M.; Waldhör, E.; Binder, H.; Kaim, W.; Fiedler, J. *Inorg. Chem.* **1995**, *34*, 4326. (b) Záliš, S.; Kaim, W.; Sarkar, B.; Duboc, C. *Chem. Monthly*, in print. (c) Schwederski, B.; Kasack, V.; Kaim, W.; Roth, E.; Jordanov, J. *Angew. Chem.* **1990**, *102*, 74; *Angew. Chem., Int. Ed. Engl.* **1990**, *29*, 78.

(46) (b) Waldhör, E.; Schwederski, B.; Kaim, W. *J. Chem. Soc., Perkin Trans. 2* **1993**, 2109.

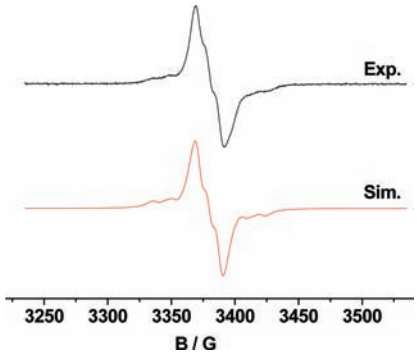

Figure 7. EPR spectrum of electrogenerated $\mathbf{2}^{o}$ at 295 K in CH_3CN/0.1 M Bu_4NPF_6, with simulation.

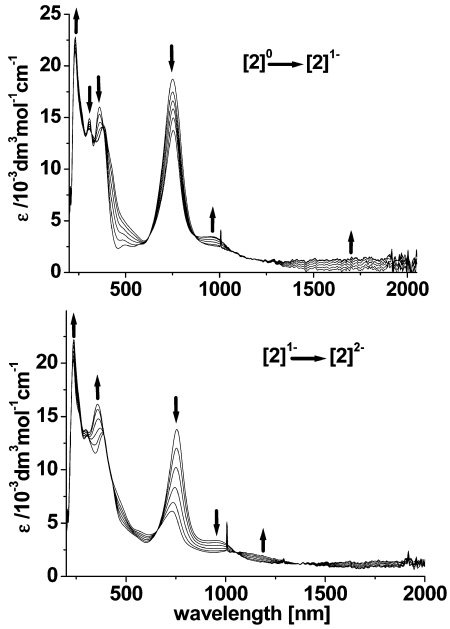

Figure 8. UV/vis/NIR-Spectroelectrochemical response of system $\mathbf{2}^{2+}$ on reduction in CH_3CN/0.1 M Bu_4NPF_6 (third and fourth step).

in the monocation. Nevertheless, the ^{14}N values are in the expected range for iminosemiquinones,[19c,47] and the $^{99,101}Ru$ satellite coupling is typical for ruthenium(II) semiquinone complexes.[40,46]

DFT calculations confirm that the first two reduction steps involve orbitals having large contributions from the Q ligands (Table S1, Figure S1). The spin density of the one-electron reduced form is calculated to be mainly delocalized over the π^* systems (Q, with smaller contributions from μ-tppz) and with little participation of Ru, as shown in Figure 5. The cumulated spin densities for $\mathbf{2}^{+}$ are 0.719, −0.097, and 0.377 for Q, Ru, and tppz, respectively.

On the third reduction a characteristic absorption appears at ca. 960 nm (Figure 8) which is typical for $tppz^{\bullet-}$.[14−14e,15] The EPR signal at $g_{iso} = 1.9987$ ($g_1 = 2.015$, $g_2 = 1.998$, $g_3 = 1.985$ at 110 K, Figure 9) without detectable metal hyperfine

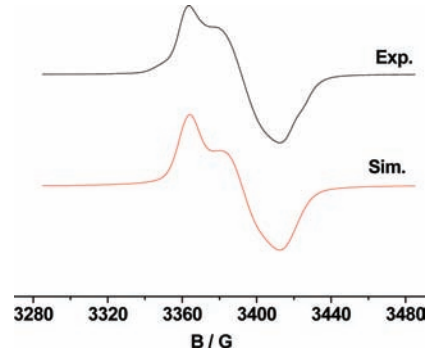

Figure 9. EPR spectrum of electrogenerated $\mathbf{2}^{-}$ at 110 K in CH_3CN/0.1 M Bu_4NPF_6, with simulation.

splitting confirms[14−14c,15] the notion of tppz-centered spin, resulting from a three-spin situation $Q^{\bullet-}$//$tppz^{\bullet-}$//$Q^{\bullet-}$ with antiparallel spin−spin interaction of the semiquinone ligands (↑↑↓). Related copper(II)-bridged bis-iminosemiquinones were discussed with respect to variable spin exchange patterns.[13,48] The fourth reduction is also believed to occur at the tppz bridge because the absorption intensity emerging at ∼1200 nm (Figure 8) has similarly been observed for other diruthenium complexes of $tppz^{2-}$.[14−14c]

Conclusion

Having combined the concepts of noninnocent ligand (NIL) behavior[49] and intramolecular electronic exchange between equivalent electron transfer sites across active bridges (BL),[1] we present a first symmetrical five-center system $[Cl(Q)Ru(\mu\text{-tppz})Ru(Q)Cl]^n$ = NIL//M//BL//M//NIL, combining two noninnocent ligand/metal (NIL/M) situations[13,49] with a classical pyrazine-bridged diruthenium configuration for mixed valency.[1,50] Starting from a structurally defined iminosemiquinonato-ruthenium(III) containing precursor, a total of six additional redox states involving $Ru^{III,II}$, $tppz^{o,\bullet-,2-}$, and $Q^{o,\bullet-,2-}$ were reversibly accessible by EPR and UV−vis−NIR spectroelectrochemistry, illustrating remarkable alternatives for intramolecular electron transfer such as mixed valency, redox-induced electron transfer, and three-spin exchange. EPR spectroelectrochemistry has turned out to be a particularly valuable tool; in agreement with DFT calculated spin densities it revealed metal-based spin for the oxidized state and various combinations of ligand-based spin for the first three reduced forms of $[Cl(Q)Ru(\mu\text{-tppz})Ru(Q)Cl](PF_6)_2$. This information has allowed us to identify the most appropriate oxidations state combinations for the individual charge forms as listed in Scheme 2. The results demonstrate that not only conventional transition metal ions,[1] nonmetal electron transfer sites,[51,52] metal clusters,[50] or bond-breaking and -reforming reaction centers[10] but also composite electron transfer moieties such as metal/noninnocent ligand entities can be electronically coupled by active bridges, adding another dimension to mixed-valence chemistry. It remains to be investigated whether even more extended and complex configurations involving noninnocent terminal or bridging ligands and electro- and spin-active metal centers can be constructed and their intramolecular spin and valence exchange behavior analyzed.

(47) Stegmann, H. B.; Ulmschneider, K. B.; Hieke, K.; Scheffler, K. *J. Organomet. Chem.* **1976**, *118*, 259.
(48) Ye, S.; Sarkar, B.; Lissner, F.; Schleid, Th.; van Slageren, J.; Fiedler, J.; Kaim, W. *Angew. Chem.* **2005**, *117*, 2140; *Angew. Chem., Int. Ed.* **2005**, *44*, 2103.
(49) Ward, M. D.; McCleverty, J. A. *J. Chem. Soc., Dalton Trans.* **2002**, 275.

Acknowledgment. Financial support from the DFG, Fonds der Chemischen Industrie and DAAD (Germany), from the DST and CSIR (New Delhi, India), and from the Grant Agency of the Academy of Sciences of the Czech Republic (KAN 100400702) and the Ministry of Education of the Czech Republic (Grant COST OC 139) is gratefully acknowledged.

Supporting Information Available: Complete ref 28 and X-ray crystallographic file in CIF format for $\mathbf{2}(PF_6)_2 \cdot (C_7H_8)$. DFT calculated MO scheme of $\mathbf{2}^+$ ion (Figure S2), composition of frontier orbitals (Table S1) and graphical representation (Figure S1), selected allowed singlet transitions (Table S2). This material is available free of charge via the Internet at http://pubs.acs.org.

JA901746X

(50) Salsman, J. C.; Ronco, S.; Londergan, C. H.; Kubiak, C. P. *Inorg. Chem.* **2006**, *45*, 547. (b) Adams, H.; Costa, P. J.; Newell, M.; Vickers, S. J.; Ward, M. D.; Félix, V.; Thomas, J. A. *Inorg. Chem.* **2008**, *47*, 11633.
(51) (a) Nelsen, S. F. *Chem.—Eur. J.* **2000**, *6*, 581. (b) Lambert, C.; Nöll, G.; Schelter, J. *Nat. Mater.* **2002**, *1*, 69.
(52) Zalis, S.; Kaim, W. *Main Group Chem.* **2007**, *6*, 267.